A Comparison of RF Exposure in Macro- and Femtocells

Brad Zarikoff and David Malone*

* Hamilton Institute, NUI Maynooth, Kildare, Ireland. Fax: +353-1-708 6296. Tel: +353-1-708 6463. Email: {Brad.Zarikoff,David.Malone}@nuim.ie. The authors are supported by SFI grant 08/SRC/I1403 and 07/SK/I1216a.

Abstract

This paper assesses radio frequency exposure of a mobile handset user in the context of a new class of cellular base station: the femtocell. Traditional cellular network construction relies on using a single base station to cover a large area and serve dozens to hundreds of users. The femtocell (named after the minuscule size of the coverage area) provides a low-power in-home cellular connection for the mobile handset. Consequently, we expect it to behave differently to a macrocell in terms of the user's radio frequency energy exposure. Our work focuses on the trade-off in incident power on the mobile handset user when connected to either a macrocell or femtocell using power loss and power control models. Contrary to many individual's initial feeling that putting a base station in your home would increase exposure, our findings indicate that having a femtocell in the home will actually reduce the mobile handset user's exposure to radio frequency energy.

Keywords

exposure, radiofrequency; safety standards; radiofrequency; standards

Introduction

Cellular network providers have recently adopted a new method of dealing with the common problem of gaps in cellular network coverage: the femtocell. A femtocell is basically a compact, low power replica of the large mast-mounted wide- and local-area base stations (BSs) that are common to cellular systems. Femtocell base stations are designed to be deployed within home and small office environments. The purpose behind a femtocell is to provide the owner with a “5 bar” signal within the home, avoiding the need for a cellular subscriber to be serviced by the wide- or local-area base station. The network provider also benefits by offsetting a proportion of traffic to the subscriber’s broadband connection and by avoiding the installation of additional wide- and local-area base stations.

From the perspective of the cellular provider, these femtocells are a perfect solution to the long-running problem of signal penetration into complex structures (such as homes and offices). From the perspective of the home user, a femtocell will almost definitely improve their home coverage and signal fidelity. However, due to a common conception that wireless devices are dangerous to individuals in close proximity (due to high transmit power levels), there is a public perception of risk in adding wireless base stations within the home (World Health Organization 2011).

There are two factors that run contrary to these fears. First, a femtocell base station is only permitted to transmit at a much lower power (125 mW for class 4 device, ICNIRP 2008) compared to the mast-mount versions (> 20 W, Arnold et al. 2010). This is similar to the power of the ubiquitous wireless local area network access points (100 mW, ICNIRP 2008). Second, the handset itself is a major contributor to the radio frequency (RF) exposure of the individual. Further, power control algorithms at both the handset and the femtocell base station may reduce the transmit power of both devices if the received signal level at each device warrants it.

In this paper, we look at the issue of femtocell RF exposure with an eye to the power control mechanism employed in the handset. We consider two mechanisms for RF exposure: from the base station (femto or macro) and from the handset. In modern handsets, a power control algorithm operates to minimize the transmit power in the hope of maximising battery life. The signal loss between the base station and the handset is continually monitored and reported to the handset, which then adapts to maintain a certain desired received signal level at the base station.

Note that this paper focuses on the case where an individual will be using a cellular handset in the home, regardless of which base station they are connecting to.

Material and Methods

Cellular networks

The original tenet of cellular communications, as first formulated in the 1950s through 1970s, utilizes the concept of frequency reuse between distant cells (Rappaport 2002). It relied on the basic physical premise of path loss (that the further away a transmitter is from a receiver, the lower the observed signal power) and that two equally-sized cells can operate at the same frequency provided they are separated with a large enough distance.

Femtocell technology provides a modern extension to the original cellular concept. By apportioning a small-sized “femto” cell within the larger macrocell network, the cellular provider can fill coverage gaps within a home and allow for a lower reuse factor (a factor that dictates how close same-channel base stations can operate). While the deployment of femtocell has been a relatively painless process (multiple carriers throughout Europe and North America already have femtocell base stations on offer for the public), there are still open questions as to how such systems will impact the cellular system as a whole. Particularly, interference between femtocells and macrocells are a hot research topic (Chandrasekhar et al. 2008, Jeney 2011, Chandrasekhar and Andrews 2009, Yavuz et al. 2009).

As a result of the introduction of femtocells, the issue of RF exposure has been raised in Koutitas and Samaras 2010 and Korinthios et al. 2009. Our work looks at an interesting twist of using a femtocell within a home: that of reduced RF exposure. Current biological research studies are still looking for more data before making any decisions on the effects of low-level recurring RF exposure (Baan et al. 2011), but such academic endeavours do not stop individuals from being concerned over health issues related to RF exposure. While the possibility that power may be reduced when the distance to the base station is small is known to the RF exposure community (ICNIRP 2008), we do not believe it has been studied in detail for femtocells.

The following section lays out an approach to calculating and contrasting the relative exposure of a cellular user in the home in the presence and absence of a femtocell. We begin by presenting the background and assumptions that we use throughout our calculations in III-A. Then we detail the radio frequency channel model that we use for path-loss estimation in III-B. A discussion of RF exposure is given in Section III-C, followed by a summary of power control in the Universal Mobile Telecommunications System (UMTS) Third Generation (3G) cellular system in III-D. Finally, we introduce our RF exposure model in III-E, which integrates elements of the preceding sections.

Assumptions and system parameters

In this work, we consider a femtocell deployed in an urban home environment in the European UMTS band (1.9-2.1 GHz). The assumption is that while a handset will have access to a macrocell base station throughout most of the home, there is a possibility that some areas will suffer from low or zero connectivity. Further, we assume that the handset is far enough from the macrocell base station to have a path-loss exponent greater than 2;

in Barbiroli et al. 2002, this distance was estimated to > 60 m, which is realistic for the majority of home scenarios.

For simplicity, we consider an isolated system, where there is a single handset plus the femtocell and macrocell base stations. Thus, we do not consider the effect of neighbouring femtocell, macrocell, or handset interference in this study. A co-channel and co-located handset incapable of associating with the femtocell under consideration (e.g. due to association control) would add to the noise floor in the UMTS channel. Such an increase would itself require path-loss modelling and a highly complex simulation. As most current deployments of femtocells are based on the UMTS 3G standard, we use the power control algorithms common to that technology. We also assume no path loss between the handset and the user, i.e. 100% of the energy emitted by the handset is absorbed by the user. This provides us with an upper bound, as obviously a lower proportion of transmit energy is absorbed (otherwise communications could not be established).

To compensate for the far-field, whole-body absorption of the femtocell and macrocell base station signals at a given location, one technique is to use an approximation of the effected cross-sectional area. Similar to the path loss assumption above between the handset and the user, a conservative approximation of the human cross-section is ~1 m^2.

Throughout the rest of this document, the convention when discussing power levels will be that lower-case letter p will correspond to power measured in Watts, and upper-case letter P will correspond to decibels referenced to 1 mW (dBm), i.e. $P = 10\log_{10}(\frac{\mathrm{p}}{1\mathrm{mW}})$. All other units will be defined as necessary.

Channel models

RF propagation was extensively studied throughout the 1980's and 1990's. Numerous RF propagation models have resulted from this research. RF signals propagate by direct path (line of sight), by refraction (around corners) and by reflection (depending on the material). Due to the complexity of the RF channel, empirical models are the tool of choice for systems research (Integrated Environmental Health Impact Assessment System 2011, Barbiroli et al. 2003), although ray-tracing and experimental measurements have been used in academic study (Koutitas and Samaras 2010, Wiart et al. 2000, Sarkar et al. 2003). The empirical models benefit from ease-of-use and generality, and so we use them in our work.

As discussed in Abhayawardhana et al. 2005 and Rappaport 2002, there are a number of empirical models to choose from for the 1.9-2.1 GHz UMTS band. Since we are considering a domestic urban scenario, we chose to use the log-distance path-loss model in Alexander 1983 and Feuerstein et al. 1994. Other more specialized models such as the popular COST 231 Hata model from Office for Official Publications of the European Communities 1999 and the ECC-33 model from Abhayawardhana et al. 2005 are limited to receiver-transmitter separation distances of greater than 1 km.

The power law model is commonly used to estimate the median power loss due to distance from the transmitter (Molkdar 1991). In this model, the path loss is a function of the distance *d* between the transmitter and receiver and a path-loss exponent *n*, where

$$L(d,n) = 10 \times n \times \log_{10} d + L(d_0), \quad (1)$$

and $L(d_0)$ is the path loss at a reference distance, usually 1 m. $L(d_0)$ is commonly calculated using the Friis transmission equation to be $L(d_0) = 20 \times \log_{10}\left(\frac{4\times\pi\times d_0}{\lambda}\right)$. For the 1.95 GHz UMTS operating band I, this means $L(d_0) = 38.25$ dB.

We require modelling of both indoor and outdoor channels, both of which scenarios have been empirically studied with the log-distance model. For the outdoor channel that would categorize our macrocell BS to handset path, the path-loss exponent was measured to be in the range of 2.58 to 2.69. These results are for an obstructed channel and depend on the height of the BS.

For the indoor channel, the path-loss exponent *n* has been measured to range from 1.2 to 6.5 (Alexander 1983), depending on the building structure and materials. The range of scatter about the path loss lines varies from 7 dB to 12 dB for the indoor of a house scenario. For our purposes, we use values of 2.2, 3.0, and 4.0 (Alexander 1983, Rappaport 2002).

Radio frequency exposure

The European Commission, the American National Standards Institute (ANSI) and the Institute of Electrical and Electronics Engineering (IEEE) have defined limits on the RF exposure for the general public (Martinez-Burdalo et al. 2009, Ahlbom et al. 1998, ANSI/IEEE 2005). The limits are frequency dependent: for the 1.9 GHz cellular band, the limits are stated in terms of the specific absorption rate (SAR), averaged over a volume containing 10 g of tissue and over any 6 minute period. The limit is measured in Watts per kilogram, and is set at 0.08 W kg^{-1} for the whole-body, 2 W kg^{-1} localized for the head and trunk, and 4 W kg^{-1} localized for the limbs. Strictly speaking, SAR is a measure of heat absorption over a specified region, after taking into account the electric conductivity (σ) and mass density (ρ) of the region. That is,

$$SAR = \int_{\mathbb{V}} \frac{\sigma \times E^2(r)}{\rho} dr, \qquad (2)$$

where $\mathbb{V}$ is the volume, E(r) is the electric field in V m^{-1}, σ is the electric conductivity in S m^{-1}, ρ is the mass density in kg m^{-3}, and SAR is measured in W kg^{-1}.

In our study, we don't measure the SAR directly, but approximate it with the received power at a distance from the transmitter. We consider the user's body as an ideal omni-directional antenna, with an effective area of 1 m^2, and so do not factor in issues of tissue conductivity, mass or non-uniform exposure. Our analysis and experiments in effect look at power observed at a given location rather than localized and whole-body absorption. Although our model is simplified, it provides a means to compare arrival powers as a function of distance between the user and a BS. We do not require exact SAR metrics for our study, since we are interested in the relative received power at the user's location. We are thus interested solely in Watts rather than Watts per kilogram.

Power control

To begin, a summary of all the variables used in the following sections is provided in Table 1. From this point on, we resort to cellular vernacular and refer to the mobile handset as the user equipment (UE). The transmit power control (TPC) algorithm for

UMTS systems is an integral part of operation, and our aim is to use it to calculate the transmit power of a handset. For instance, when multiple users are connected to a base station, it is essential to have the uplink signals (from the handset to the base station) arrive at similar power levels because of technical requirements of the code division multiple access (CDMA) protocol (Gilhousen et al. 1991) used in UMTS systems. Further, to conserve battery power, a handset is optimized to transmit at the lowest level possible.

In UMTS, the TPC algorithm is dependent on whether the system is operating in frequency division duplex (FDD) or time division duplex (TDD) mode. For FDD, the TPC operates as a closed-loop system, which is required since the channel is not symmetric (Baker and Mouslsley 2000). Briefly, the system operates with an inner-loop, to compensate for short term channel fluctuations, and an outer-loop, to compensate for longer term variations. The base station measures the received power from a handset, and provides feedback to the handset to either increase or decrease its transmit power. This feedback serves to continuously adjust the power levels until the system converges to a satisfactory steady state. For TDD, the channel can be viewed as symmetric in both uplink and downlink, and therefore an open-loop power control approach can be used, as described in Kurjenniemi et al. 2001.

Next, we consider both the UMTS FDD and TDD TPC algorithms and show that after applying a few principled assumptions, they can be considered to be identical. First, consider that the outer-loop of the FDD TPC was designed to compensate for both shadowing (severe signal attenuation due to some large obstruction) and variable interference levels. We propose here that in a femtocell, the TPC algorithm can be simplified. Interferers will be largely absent within a domestic femtocell (e.g. imagine a low-power cell with only one or two handsets and the requisite control channels). Furthermore, shadowing will not be a problem, since a general in-home setting will consist of relatively low-loss walls. Hence, we assume that the outer loop will be largely inactive, and we can simplify the FDD TPC algorithm to consider only the inner loop.

The inner loop of the TPC algorithm focuses on the signal to interference and noise ratio (SINR). The measured SINR at the base station is

$$SINR_{est} = P_{UE,tx} - L_{UL} - IN_{BS}, \tag{3}$$

that is, the transmission power from the UE ($P_{UE,tx}$) less the path loss in the uplink channel (L_{UL}) and the interference plus noise power (IN_{BS}) resulting from thermal noise and in-band interferers. Then when the power control algorithm converges, the handset transmit power is

$$P_{UE,tx}^{FDD} = SINR_{target} + L_{UL} + IN_{BS}, \tag{4}$$

where $SINR_{target}$ is the target SINR at the BS to achieve some predetermined bit error rate. Similarly, for TDD power control as in 3GPP 2011b, we have

$$P_{UE,tx}^{FDD} = SINR_{target} + \gamma \times L_{UL} + (1-\gamma) \times L_0 + IN_{BS} + C, \tag{5}$$

where $\gamma \in [0,1]$ is a weighting parameter based on the quality of the L_{UL} estimates, L_0 is the measured mean path loss, and C is some higher layer constant value that depends on the type of channel in use. This expression is identical to our simplified FDD expression if we trust the path loss estimate ($\gamma = 1$) and set $C = 0$. Finally, if we substitute $SINR_{target} = P_{BS,0} - IN_{BS}$, where $P_{BS,0}$ is the desired receive level (sensitivity) at the base station in dBm, and include a maximum and minimum transmit power of the handset, then we have for both TDD and FDD

$$P_{UE,tx} = \max\left(\min\left(P_{UE,max}, P_{BS,0} + L_{UL}\right), P_{UE,min}\right), \quad (6)$$

where $P_{UE,max}$ and $P_{UE,min}$ are the maximum and minimum transmit powers of the handset. Note that values of $P_{BS,0}$ vary between femtocells and macrocells. We assume that the desired receive level remains fixed, although in general it will be dependent on the current modulation and coding level selected.

Model-based approximation for RF exposure

We suggest that the power incident on a cellular handset user can be broken down into the following parts. The average power incident on an individual, p_{user}, is dependent on:

- $p_{UE,tx}$ is the power transmitted by the UE,
- $p_{BS,tx}$ is the power transmitted by the BS to the UE,
- L_{BS} is the path loss between the BS and the UE,
- α is the overhead coefficient (for BS discovery, synchronisation, etc.), and
- β the proportion of time spent in an active call.

The last two components have to do with the dynamics of call-specific transmissions and constant overhead BS radiation (e.g. pilot and synchronization channels). Then, for a connection with a macrocell base station (MBS),

$$p_{user}^{(macro)} = p_{UE,tx}^{(macro)} \times \beta + p_{MBS,tx} \times A \times 10^{-\frac{L_{MBS}}{10}} \times (\alpha + \beta),$$

(7)

where the first term is the power incident from the UE to the user, the second term is the power incident from the MBS to the user, L_{MBS} is the path loss between the MBS and the

UE and $A = 1\ m^2$ is the unitary cross-section . Similarly, for a connection with a femtocell BS (FBS),

$$p_{user}^{(femto)} = p_{UE,tx}^{(femto)} \times \beta + p_{MBS,tx} \times A \times 10^{-\frac{L^{(macro)}}{10}} \times \alpha +$$

$$p_{FBS,tx} \times A \times 10^{-\frac{L_{FBS}}{10}} \times (\alpha + \beta), \tag{8}$$

where the first term is the power incident from the UE to the user, the second term is the power incident from the MBS to the user with path loss $L^{(macro)}$, and the third term is the power incident from the FBS to the user with path loss L_{FBS}. We include this second term since the MBS background radiation is present regardless of the presence of the femtocell. Finally, we make the assumption that $p_{BS,tx} = p_{BS,max}$, which provides an upper bound for our exposure estimates. This is justified by there being no mandatory requirement for the BS to respond to the TPC requests from a handset (Baker and Mouslsley 2000).

Using this model, we can find the distance from the BS that will minimize the upper bound to the exposure p_{user}. That is, find $d_{min} = \min_d p_{user}(d)$. After replacing $p_{UE,tx} = p_{BS,0} 10^{-\frac{L_{UL}}{10}}$ using (6), this works out to be

$$d_{min} = \sqrt[2\times n]{\frac{p_{BS,tx} \times (\alpha+\beta) \times 10^{-2\times 3.825}}{p_{BS,0} \times \beta}}, \tag{9}$$

where the $10^{-2\times 3.825}$ term comes straight from the path loss expression (from (1), $10^{-\frac{L}{10}} = 10^{-\frac{10 n log_{10} d + 38.25}{10}} = d^{-n} 10^{-3.825}$, with both the UE and BS contributing). Calculation of d_{min} is the same for both MBS and FBS scenarios if we assume that the macrocell is far enough away that we can approximate it to be at a fixed distance D_m from the UE.

Results

Our goal is to compare the RF exposure of a mobile handset user with and without a femtocell in the home environment using our estimates of the power incident on a user as derived above. We use the power received by an ideal antenna to compare relative measures of RF exposure. The distance between the UE and the MBS is denoted as d_m, and the distance between the UE to the FBS is denoted as d_f . Note that the femtocell-related curves show distance to the femtocell, while the macrocell related curves show distance to the macrocell.

In order to compare and contrast the effective RF exposure due to an active call and to the continuous background radiation emitted by a femtocell, we consider four scenarios as follows:

1. No femtocell present, 24 hour average
2. Femtocell present, 24 hour average
3. No femtocell present, 3.29 minute average
4. Femtocell present, 3.29 minute average

The 3.29 minute average is based on the average duration of a single call, as reported in Bridge Ratings 2011. For the 24 hour average, we take an indicative example and assume that there are 5 calls day^{-1} (Lehnert 2010), each duration 3.29 minutes, so 16.45 minutes day^{-1}. For the 3.29 minute call, we assume that a call is active for the duration. Note that this is close to the 6 minute period used by the ICNIRP for averaging (ICNIRP 2008).

To generate the exposure curves for these scenarios, we parameterise the RF power exposure expressions in (7) and (8) on the distance to the active BS, d. The pathloss L_{BS} between the active BS and handset is modelled using (1), while the transmit power of the handset $p_{UE,tx}$ is from (6). The value of β depends on the scenario, while α and L_{MBS} (for the femtocell case) have values justified in Section IV-B.

Experiments

In order to verify the power control functionality of a commodity handset, we ran some experiments using a Nokia X6 using the Vodafone network in Ireland, in and out of the vicinity of a femtocell. The Vodafone 3G uplink channels are in the 1950 to 1965 MHz range (Vodafone Ireland 2011). For the femtocell experiment, we attached a patch antenna onto the back of the handset: while we acknowledge that this will not provide an accurate measure of the *true* RF transmit power, in the context of measurements at different locations and distances, it provides a good estimate of the power control functionality of the handset. The antenna was connected to a Rohde & Schwarz FSL-6 spectrum analyzer. Fig. 1 shows the results of the transmission from the handset when connected to the FBS within the home. The spectrum analyzer was set up with settings in Table 2 and 10 measurements were taken at points from 1 m to 10 m: the measurements from 1 m to 8 m were done with a strong line-of-sight component. Using a simple least squares fit, the estimate for path-loss exponent n is found to be $\hat{n} = 3.15$. This value fits well within the expected range, and it is clear from these results that the handset implements power control as expected. An additional experiment was done with the handset connected to the MBS within an office, using a number of measurements at various points. It shows that the spread in the handset transmission power (≈ 75 dB) is much larger than for the FBS case, that the MBS has a larger dynamic range and a lower sensitivity level, and thus must deal with a more diverse channel than FBSs.

As mentioned previously, we assume that a FBS and MBS do not respond to TPC commands and thus constantly transmit at maximum power. We conducted an experiment to check this assumption with respect to the FBS and to verify the path-loss exponent for a small or home office environment. Fig. 2 shows transmit signal strength measurements of the FBS at distances of up to 15 m within a small office. The spectrum analyzer was setup with settings in Table 3. Each distance has from two to five measurement points, with both measurements and the average plotted. Using a simple least squares fit, the estimate for path-loss exponent n is found to be $\hat{n} = 2.04$. Again, this value fits well within the expected range as the experimental setup is close to line-of-sight with some surrounding reflections.

Simulations

With experimental results which confirm that mobile handsets perform power control and have a wide range of transmit powers, we now use the model developed in Section III to explore relative RF exposure. Consider Fig. 3 and 4, which show the power incident at a user averaged over a day or a call (3.29 minutes). The darker curves in each figure shows incident power with a femtocell and the lighter curve without. We assume that $\alpha \approx 0.1$ because of the common pilot channel (CPICH) and synchronization channel (SCH), which are detailed in Su 2007. Also, for the femtocell curves (dark), the background radiation contribution from the MBS is approximated using $d_m = 100$ m. However, using our model, it is clear that the contribution $p_{BS,tx}^{(macro)}$ to the femtocell scenario is relatively inconsequential. Note that we see comparable results for the 6 minutes period required in SAR measurements, which corresponds to a slight shift in the location of d_{min} and in the maximum exposure level when d is large.

The bold section of each curve corresponds to a typical range of distance from BS and UE, so $d_f \in [1{,}50]$ m and $d_m \in [30{,}1500]$ m. While the typical range for the FBS is based on its location in a room within a home, the MBS range is based on the physical constraints that i) the antenna is located on a mast or on a tall building, and that ii) the BS density will restrict the distance to a closer BS to less than a few kilometres in an urban setting. To verify this range, we took samples of BS locations at specific geographic positions within residential areas of Dublin, Ireland, and then averaged over uniformly sampled random locations to find the average distance to the closest BS. The results indicate an average distance of 150 m to 300 m, with Table 4 giving more detail. When considering cities in North America, we suspect that the average distance will be larger because of the comparatively lower density of the urban and sub-urban areas.

For the 24 hour experiment, an individual at a distance $d_f < 15$ m from the FBS, assuming a path-loss exponent $n < 3.0$, could expect an average exposure less than -23 dBm. If the same individual did not have a femtocell in their home, then in order to limit the exposure to the same level, they would need to be within a distance of approximately 30 m to a MBS. Since most macrocell sites are mast-mounted, this is a prohibitively close distance, and most users would most likely be in the hundreds of metres.

Comparing the simulations in Fig. 3 and Fig. 4, the most significant difference between the two plots is simply a vertical shift of the curves. This indicates that the contribution from the background RF energy amortized over a day proves to be small. There is a slight shift in the minimums to the left for the shorter experiment, on account of the lesser contribution from the base station to the average power.

For the parameters shown, the minimum point d_{min} from (9) is easily seen for all curves. For $d < d_{min}$, the dominant exposure mechanism is the MBS/FBS transmit power, while for $d > d_{min}$, it is the TPC of the UE. For the macrocell case, $d_{min}^{(macro)} = 13.62$ m for the 24 hour test and 9.07 m for the 3.29 minute test. The maximum $P_{user}^{(macro)}$ results from the MBS being far enough away from the UE that the UE TPC algorithm requires the maximum value, and is $P_{user}^{(macro)} \approx P_{UE,max} + 10 \times \log_{10}\beta$.

For the femtocell curves, we compare multiple path-loss exponents. The variation in d_{min} is a combination of all system components, as defined in (9). In general, by increasing the path-loss exponent, d_{min} will decrease. This corresponds to the UE needing to increase it's transmit power to accommodate for the increased path loss. The location of the inflection point in effect defines the area where the exposure from the handset is minimised. For example, in the 24 hour test, the RF exposure is expected to be the same at a distance of 1 m of the FBS or at a distance of 5.5, 10 and 21 m, for $n = 4.0$, 3.0, and 2.2, respectively, with all points between having a lower RF exposure. Note that our model assumes that there is a minimum 38.25 dB attenuation between either BS or the UE (from the 1 m reference distance), while for the handset there is no minimum attenuation. However, we consider this appropriate given that the UE will be located directly next to the user's body, while the BS will always be at a distance of at least a few metres.

The effect of the transmit power limit is fixed by individual cellular standards; however the effect of changing these limits is easily seen in our model. For example, changing the maximum transmit power of the handset will shift the level at which the power saturates as we move away from the base station.

Fig. 5 shows the relative contribution to P_{user} from each of UE, FBS and MBS at seven distances: $1\ m$, $2\ m$, $3\ m$, $4\ m$, $5\ m$, $10\ m$ and $15\ m$. These points correspond to the single call average (Fig. 4) and show that the FBS contribution is greater than the UE contribution when the distance between the UE and the FBS is less than $3\ m$ and vice versa when the distance is greater than $3\ m$. Note that in this example, the MBS contribution is dwarfed by the FBS and UE contributions. The conclusion here again is that it is the UE contribution that is of most importance when gauging the RF exposure at the user's location. Of course, a different biological impact may result from the localised nature of the UE's exposure compared to the more even exposure caused by the femtocell.

A further simple example can be used to illustrate the relation between $\mathrm{p_{user}}$ and SAR using the data from Fig. 5. Suppose over the averaging period the power from the handset is spread over $100\ g$ of head/torso tissue of an $80\ kg$ adult. SAR due to the femtocell/macrocell base station could be estimated as $(p_{user,femto} + p_{user,macro})/$ $80\ kg$ and the additional dose to the head/torso tissue from the handset could be estimated as $(p_{user,UE})/0.1\ kg$. For instance, using Fig. 5 at a distance of $3\ m$, we calculate a SAR estimate of $0.00002\ W\ kg^{-1}$ for the $80\ kg$ whole-body and

$0.015\ W\ kg^{-1}$ for the $100\ g$ of head/torso. Naturally, more sophisticated SAR models could be used, if required.

Discussion

Throughout this work, we have made a number of simplifying assumptions. These have allowed us to combine two relatively simple models, TPC and path loss, for the sake of estimating relative RF exposure levels. In summary, we have assumed that the TPC in UMTS systems is operating with a constant target, that the path loss will behave on average in a manner consistent with the empirical models, and that the required receive sensitivity level is fixed. It is our view that these approximations do not detract from the comparison of the femtocell scenario versus the macrocell scenario, since each approximation is applied to each.

The primary uncertainty in our simulations falls on the path loss of the radio channel, and therefore on the instantaneous path-loss exponent. In (Alexander 1983), the scatter of measured data points around the extrapolated path-loss gradient ranged from 1 dB (for an aircraft hangar) to 16 dB (for an office block). For a house, the scatter was found to range from 7 to 12 dB: for our simulations, this would translate to a horizontal shift of the curves in Fig. 3 through 5 with similar magnitudes. The inclusion of additional noise in the channel due to co-channel and co-located radio users also adds to the uncertainty. While further study is required to determine the magnitude of impact, we believe it will be minimal in a typical femtocell installation.

In terms of the RF exposure, it is clear from the simulations that the maximum incident power or RF exposure is less in the case of the femtocell, primarily because of the smaller distance from the handset when compared to the macrocell and the similar target signal mean power (-81 dBm for the MBS and -77 dBm for the FBS).

For long-term exposure simulations (24 hour test), and considering typical separation distances between the handset and the BS, the femtocell scenario provides lower exposure if the user is standing less than 8 m away. This is true for any of the considered in-building fading scenarios.

When examining long-term exposure simulations (24 hour test), for typical separation distances we can consider when the femtocell scenario provides lower exposure than the *minimum* macrocell exposure. For our in-building scenarios with high path loss ($n = 4.0$), the femtocell provides lower exposure if the user is standing less than 8 m away. This range increases as the path loss decreases. As it could be expected that an individual would generally operate at a distance of a few metres from their in-building FBS, this shows that it should be expected that the individual would be subject to less RF exposure. For short-term exposure simulations (3 minute test), the same value of 8 m holds, with the difference being the location of the minimum exposure for both femtocell and macrocell scenario.

It should be kept in mind that the 8 m limit is chosen for the minimum incident power over the typical separation distances d_m in the macrocell case. This means a separation of 30 m between the user and BS. A more realistic value may be on the order of $d_m > 150$ m, in which case the incident power is close to saturation. The range of lower exposure when connected to a FBS will expand, e.g. for $d_m = 150$ m, the femtocell scenario provides lower exposure if the user is standing less than 20 m away.

To recast this exposure comparison in an everyday context, consider the following examples with more realistic sample values:

1. The owner of a small 10×15 m bungalow suffers from dropped calls as they move from their living room to their kitchen. They have checked with their service provider, and it appears that the nearest base station is 400 m away. Assuming a path-loss exponent of $n = 2.69$, their average RF exposure over the course of a day is estimated to be 21 dBm. After installing a femtocell base station above the top of a bookshelf in their living room, the call drops have completely disappeared. Given the dimensions of the bungalow, the furthest from the femtocell BS the handset could be is 18 m. Assuming an indoor path-loss exponent of $n = 3$, the owners RF exposure has dropped to -1 dBm, a factor of over 150 times.
2. The owner of a large two-floor 20×20 m house has adequate cellular coverage throughout the home, but does notice some signal quality degradation when moving around the house. The nearest base station is only 150 m away. Assuming a path-loss exponent of $n = 2.69$, their average RF exposure over the course of a day is estimated to be 15.79 dBm. After installing a femtocell to improve their reception, with a path-loss exponent of $n = 3.2$ and a floor height of 3 m (maximum separation from femtocell BS is then 28.44 m), the owners RF exposure has dropped to 7.75 dBm, a factor of over 6 times.

While the path-loss exponent n and its variation throughout a household will vary in a real-world situation, they are indicative of typical values and are empirically-derived.

In this paper, we have presented a framework for gauging the relative benefit of new femtocell technology in terms of an individual's RF exposure. Our model is a combination of accepted empirical channel models and the standardised power control mechanism used in common-place cellular devices, which was explored via experimental results. In general, our results demonstrate that only in cases of excessive distance between the mobile user and the femtocell will the user experience more exposure then if connected to the macrocell.

In conclusion, this contribution is useful for system planners and groups that are seeking to minimize RF exposure. The expressions used to generate the simulated results are compact and easy-to-use, and only require an estimated path-loss exponent and the distances between the mobile user and the base station.

References

3GPP. Universal Mobile Telecommunications System (UMTS); Base Station radio transmission and reception (FDD). Sophia Antipolis, France: European Telecommunications Standards Institute; 3GPP TS 125.104 V10.1.0; 2011.

3GPP. Universal Mobile Telecommunications System (UMTS); Radio Resource Control (RRC); Protocol specification. Sophia Antipolis, France: European Telecommunications Standards Institute; TS 125.331 V10.3.1; 2011.

3GPP. Universal Mobile Telecommunications System (UMTS); User Equipment (UE) radio transmission and reception (FDD). Sophia Antipolis, France: European Telecommunications Standards Institute; TS 25.101 V10.0.1; 2011.

Abhayawardhana VS, Wassell IJ, Crosby D, Sellars MP, Brown MG. Comparison of empirical propagation path loss models for fixed wireless access systems. Proceedings of the IEEE 61st Vehicular Technology Conference (VTC). Stockholm: IEEE; 2005; 73-77.

Ahlbom A, Bergqvist U, Bernhardt JH, Cesarini Jp, Court LA, Grandolfo M, Hietanen M, Mckinlay AF, Repacholi MH, Sliney DH, Stolwijk JAJ, Swicord ML, Szabo LD, Taki M, Tenforde TS, Jammet HP, Matthes R. Guidelines for limiting exposure to time-varying electric, magnetic, and electromagnetic fields (up to 300 GHz). International Commission on Non-Ionizing Radiation Protection. Health Phys 74(4):494–522; 1998.

Alexander SE. Characterising buildings for propagation at 900 MHz. Electronics Letters 19(20):860; 1983.

American National Standards Institute (ANSI)/IEEE. IEEE Standard for Safety Levels with Respect to Human Exposure to Radio Frequency Electromagnetic Fields, 3 kHz to 300 GHz ANSI/IEEE Standard C.95.1. New York: The Institude of Electrical and Electronics Engineers (IEEE) Inc.; 2005.

Arnold O, Richter F, Fettweis G, Blume O. Power consumption modeling of different base station types in heterogeneous cellular networks. Proceedings of the Future Network and Mobile Summit. Florence: IEEE; 2010: 1-8.

Baan R, Grosse Y, Lauby-Secretan B, El Ghissassi F, Bouvard V, Benbrahim-Tallaa L, Guha N, Islami F, Galichet L, Straif K. Carcinogenicity of radiofrequency electromagnetic fields. The Lancet Oncol 12(7):624-626; 2011.

Baker MPJ, Mouslsley TJ. Power control in UMTS Release '99. Proceedings of the 1st Int. Conf. on 3G Mobile Communication Technologies (IC3G). London: IEEE; 2000; 36-40.

Barbiroli M, Carciofi C, Degli-Esposti V, Falciasecca G. Evaluation of exposure levels generated by cellular systems: methodology and results. IEEE Trans on Vehicular Technology 51(6):1322-1329; 2002.

Bridge Ratings, LLC. Bridge Ratings Industry Study: In-Car Cell Phone Use [online]. Available at: http://www.bridgeratings.com/press_02202006-cellphone%20incar.htm. Accessed 15 September 2011.

Chandrasekhar V, Andrews J. Uplink capacity and interference avoidance for two-tier femtocell networks. IEEE Trans on Wireless Communications 8(7):3498-3509; 2009.

Chandrasekhar V, Andrews J, Gatherer A. Femtocell networks: a survey. IEEE Communications Magazine 46(9):59-67; 2008.

Commission for Communications Regulation. Mobile Sites; Base Stations and Masts [online]. Available online at: http://www.askcomreg.ie/mobile/View Mobile Sites.36.LE.asp. Accessed 30 September 2011.

Feuerstein MJ, Blackard KL, Rappaport TS, Seidel SY, Xia HH. Path loss, delay spread, and outage models as functions of antenna height for microcellular system design. IEEE Trans on Vehicular Technology 43(3):487-498; 1994.

Gilhousen KS, Jacobs IM, Padovani R, Viterbi AJ, Weaver LA Jr, Wheatley, CE III. On the capacity of a cellular CDMA system. IEEE Trans Vehicular Technology 40(2):303-312; 1991.

Integrated Environmental Health Impact Assessment System. EMF Path Loss Models [online]. Available at: http://www.integrated-assessment.eu/guidebook/emf_path_loss_models. Accessed 15 September 2011.

International Commission on Non-Ionizing Radiation Protection. ICNIRP Statement on EMF-emitting new technologies. Health Phys 94(4):376-392; 2008.

Jeney G. Practical Limits of Femtocells in a Realistic Environment. Proceedings of the IEEE 73rd Vehicular Technology Conference (VTC). Budapest: IEEE; 2011; 1-5.

Korinthios G, Theodoropoulou E, Marouda N, Mesogiti I, Nikolitsa E, Lyberopoulos G. Early experiences and lessons learned from femtocells. IEEE Communications Magazine 47(9):124-130; 2009.

Koutitas G, Samaras T. Exposure Minimization in Indoor Wireless Networks. IEEE Antennas and Wireless Propagation Letters 9:199-202; 2010.

Kurjenniemi J, Hamalainen S, Ristaniemi T. Uplink power control in UTRA TDD. Proceedings of the IEEE Int. Conf. On Communications (ICC). Helsinki: IEEE ; 2001; 1522-1527.

Lehnert A. Cell phones and American adults. Washington: Pew Research Center; 2010.

Martinez-Burdalo M, Martin A, Sanchis A, Villar R. FDTD assessment of human exposure to electromagnetic fields from WiFi and bluetooth devices in some operating situations. Bioelectromagnetics 30(2):142-151; 2009.

Molkdar D. Review on radio propagation into and within buildings. IEE Proceedings on Microwaves, Antennas and Propagation 138(1):61-73; 1991.

Office for Official Publications of the European Communities. COST Action 231, Digital Mobile Radio Towards Future Generation Systems, (Final Report). Brussels, Belgium; 1999.

Rappaport TS. Wireless Communications: Principles and Practice, 2nd ed. Englewood Cliffs, NJ: Prentice Hall; 2002.

Sarkar TK, Ji Z, Kim K, Medouri A, Salazar-Palma M. A survey of various propagation models for mobile communication. IEEE Antennas and Propagation Magazine 45(3):51-82; 2003.

Su SF. The UMTS air-interface in RF engineering: design and operation of UMTS networks, 1st ed. New York: McGraw-Hill Professional; 2007.

Vodafone Ireland. Network Interface Publication [online]. Available online at: http://www.vodafone.ie/aboutus/vfirl/network/. Accessed 15 September 2011.

Wiart J, Dale C, Bosisio AV, Le Cornec A. Analysis of the influence of the power control and discontinuous transmission on RF exposure with GSM mobile phones. IEEE Tran on Electromagnetic Compatibility 42(4):376-385; 2000.

World Health Organization. Electromagnetic fields and public health [online]. Available online at: http://www.who.int/mediacentre/factsheets/fs304/en/index.html. Accessed 1 September 2011.

Yavuz M, Meshkati F, Nanda S, Pokhariyal A, Johnson N, Raghothaman B, Richardson A. Interference management and performance analysis of UMTS/HSPA+ femtocells. IEEE Communications Magazine 47(9):102-109; 2009.

Figure captions – figures have been uploaded separately.

Figure 1: Peak power values (RMS detector) versus distance for a femtocell connection, with the handset as the transmitter. An estimate of the path-loss exponent n is calculated using a non-linear least squares solver, and found to be $\hat{n} = 3.15$.

Figure 2: Peak power values (RMS detector) versus location for a femtocell as the transmitter, in a small office environment. An estimate of the path-loss exponent n is calculated using a non-linear least squares solver, and found to $\hat{n} = 2.04$.

Figure 3: Distance between BS and handset versus P_{user}. 24 hour average ($T = 24$ hours), UE connecting to femto or macro cell, 5 average length calls ($T_{UE} = 16.45$ minutes), $\beta = T_{UE}/T \approx 0.0114$. Bold lines indicate the typical range: $[0{,}50]$ m for femtocells and $[30{,}1500]$ m for macrocells.

Figure 4: Distance between BS and handset versus P_{user}. 3.29 minute average ($T = 3.29$ minutes), UE connecting to femto or macro cell, UE transmitting constantly, call is in progress ($T_{UE} = 3.29$ minutes), $\beta = \frac{T_{UE}}{T} = 1$.

Figure 5: Comparison of P_{user} components at seven distances: $1\ m$, $2\ m$, $3\ m$, $4\ m$, $5\ m$, $10\ m$, and $15\ m$. Data is shown with a linear scale and from the 3.29 minute average example shown in Fig. 4.

Table 1: Summary of variables.

Variable Name	Description
P_{user} (dBm)	Power incident at the users location
$P_{UE,tx}$ (dBm)	Power transmitted from the handset
$P_{UE,max} = 21$ dBm	Maximum transmit power from a class 4 handset (3GPP 2011c)
$P_{UE,min} = -50$ dBm	Minimum transmit power from a handset (3GPP 2011c)
$P_{MBS,tx}$ (dBm)	Power transmitted from the macro base station
$P_{FBS,tx}$ (dBm)	Power transmitted from the femto base station
$P_{MBS,max} = 46$ dBm	Maximum transmit power from the macro base station (Arnold et al. 2010)
$P_{FBS,max} = 20$ dBm	Maximum transmit power from the femto base station (3GPP 2011a)
$P_{MBS,0} = -81$ dBm	Wanted signal mean power at a macro base station (3GPP 2011a)
$P_{FBS,0} = -77$ dBm	Wanted signal mean power at a femto base station (3GPP 2011a)
L (dB)	Path loss between the BS and UE
α	Proportion of time that a base station spends transmitting in the absence of any active connection
β	Proportion of time spent in an active call state

Table 2: Spectrum analyser settings for home experiment (UMTS uplink).

Setting	Value
Resolution bandwidth	10 kHz
Video bandwidth	30 kHz
Centre frequency	1950 MHz
Scanning bandwidth	20 MHz
Detector	RMS, max hold
Sweep time	200 ms

Table 3: Spectrum analyser settings for small office experiment (UMTS downlink).

Setting	Value
Resolution bandwidth	300 kHz
Video bandwidth	1 MHz
Centre frequency	2142.5 MHz
Scanning bandwidth	10 MHz
Detector	RMS, max hold
Sweep time	10 ms

Table 4: Average minimum distance between random locations and MBSs in three Dublin residential neighbourhoods. BS locations are based on records from the ComReg Siteviewer Service (Commission for Communications Regulation 2011). Since the locations are generated in a uniform random manner, these values are indicative only, as inappropriate locations may be used in the average (*i.e.* underneath a BS mast or in an inaccessible area).

Location	Size of Sample Area (km^2)	Number of BSs in Sample Area	$\mathbb{E}[d_m]$ (m)	$\sqrt{\mathbb{E}[(d_m^2 - \mathbb{E}[d_m])^2]}$ (m)
North of Connolly Station	0.69	15	150.66	72.64
West of Lower Drumcondra Road	0.48	7	287.23	134.88
Donnybrook & Sandymount	9.66	58	320.73	206.70

Figure 1

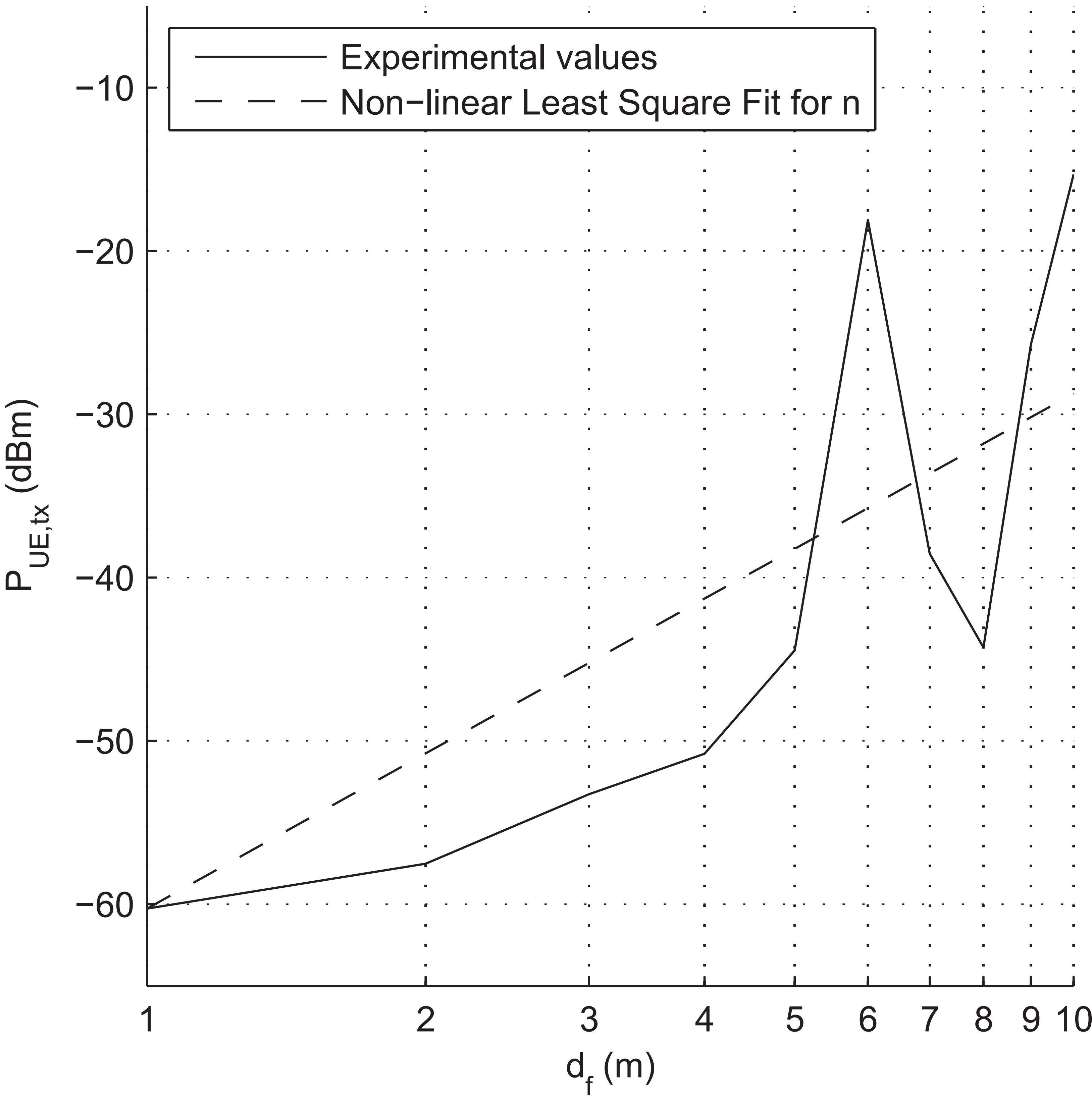

Experimental values
Non−linear Least Square Fit for n
−10
−20
−30
−40
−50
−60
$P_{UE,tx}$ (dBm)
1
2
3
4
5
6
7
8
9
10
d_f (m)

Figure 2

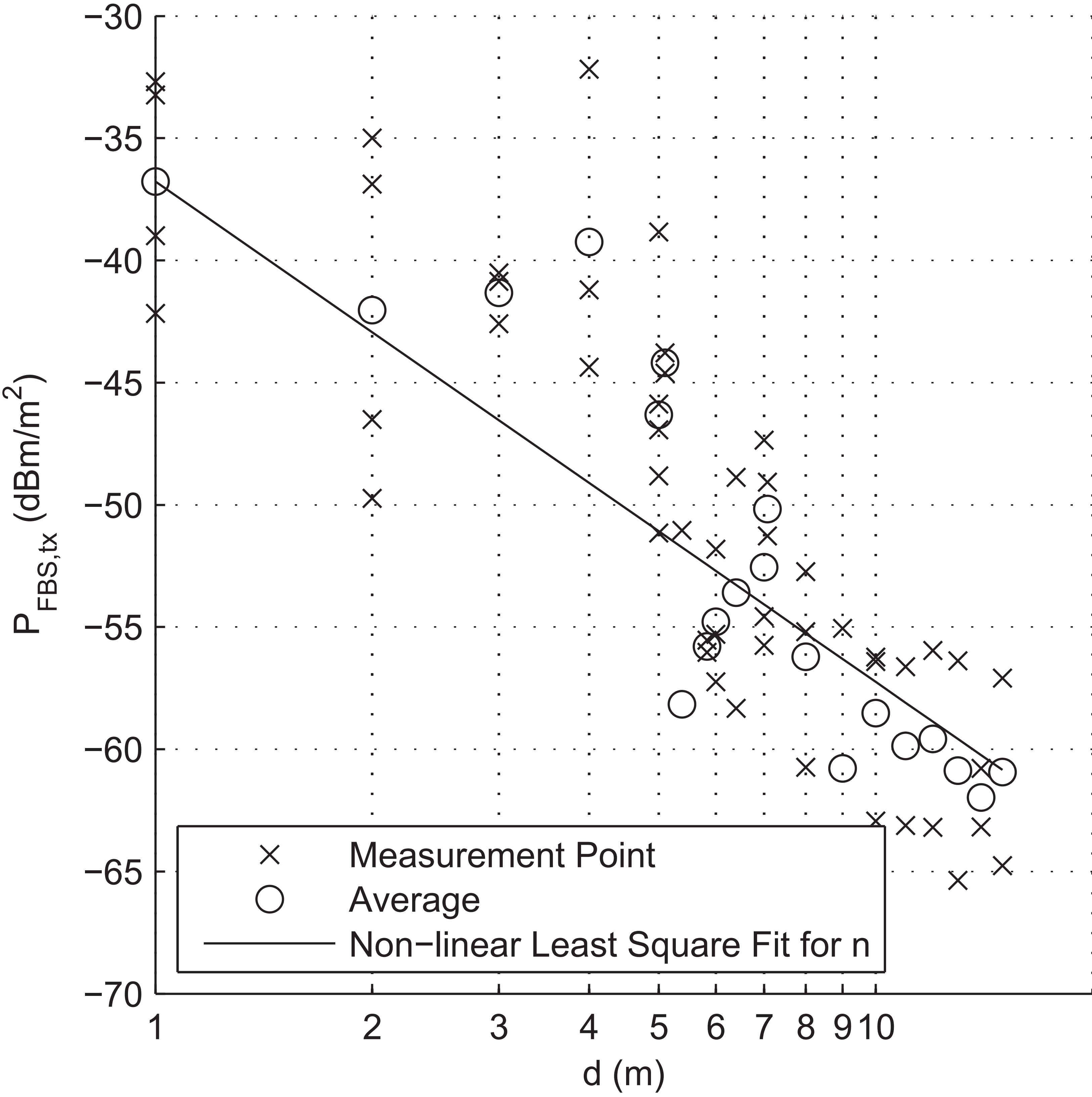

−30
−35
−40
−45
−50
−55
−60
−65
−70
$P_{FBS,tx}$ (dBm/m^2)
1
2
3
4
5
6
7
8
9
10
d (m)
Measurement Point
Average
Non−linear Least Square Fit for n

Figure 3

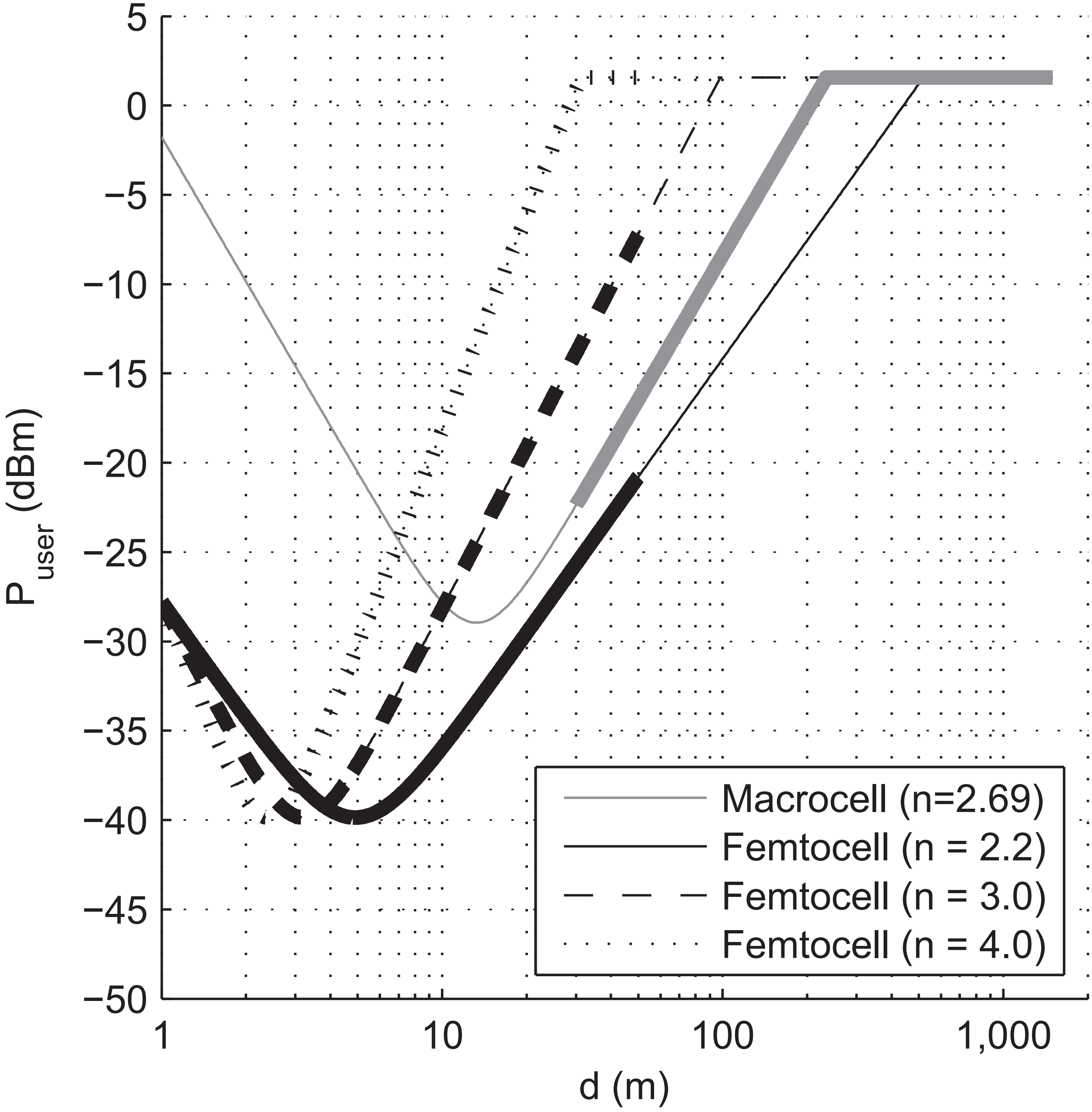

5
0
−5
−10
−15
−20
−25
−30
−35
−40
−45
−50
P_user (dBm)
1
10
100
1,000
d (m)
Macrocell (n=2.69)
Femtocell (n = 2.2)
Femtocell (n = 3.0)
Femtocell (n = 4.0)

Figure 4

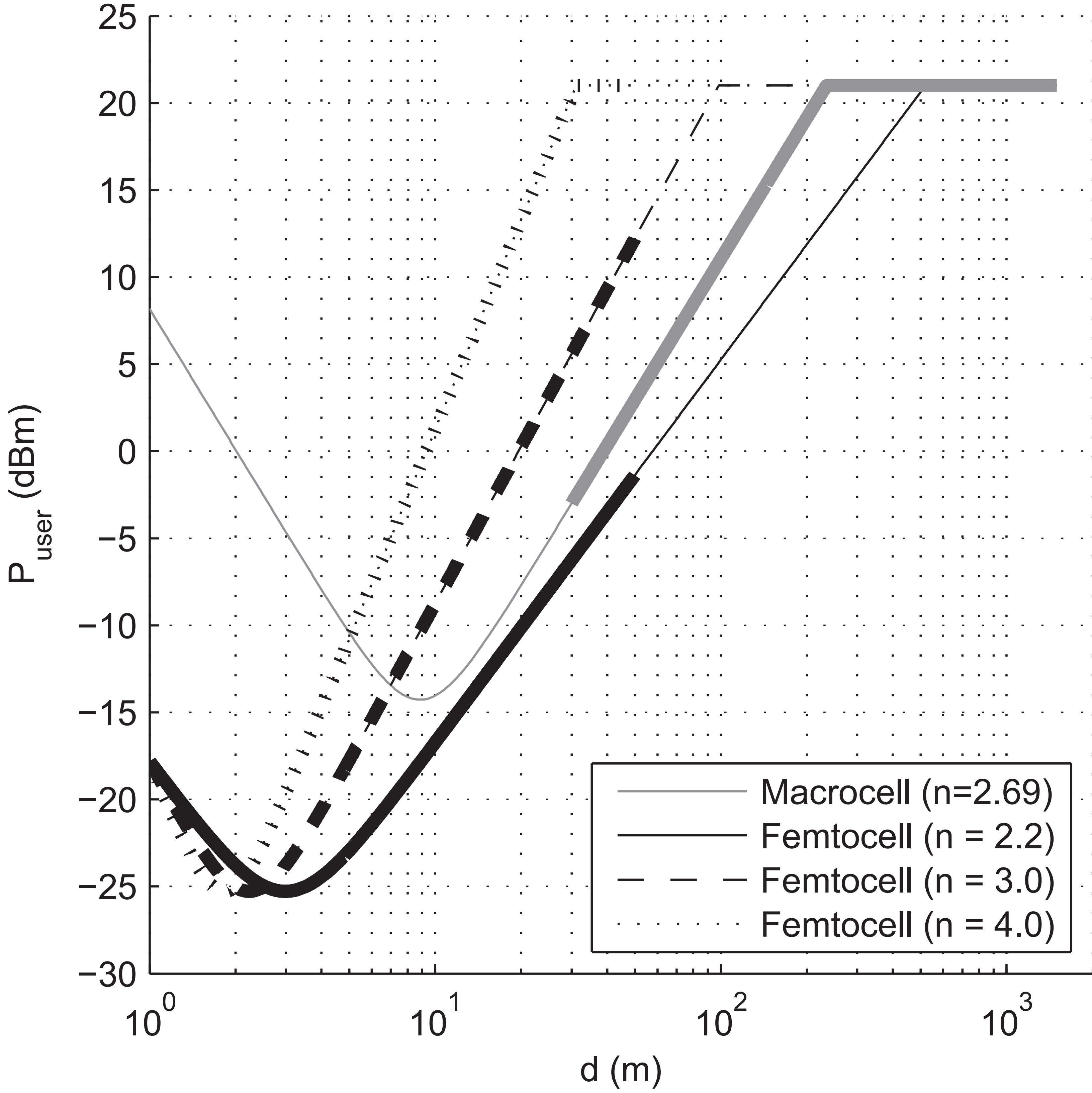

25
20
15
10
5
0
−5
−10
−15
−20
−25
−30
P_{user} (dBm)
10^0
10^1
10^2
10^3
d (m)
Macrocell (n=2.69)
Femtocell (n = 2.2)
Femtocell (n = 3.0)
Femtocell (n = 4.0)

Figure 5

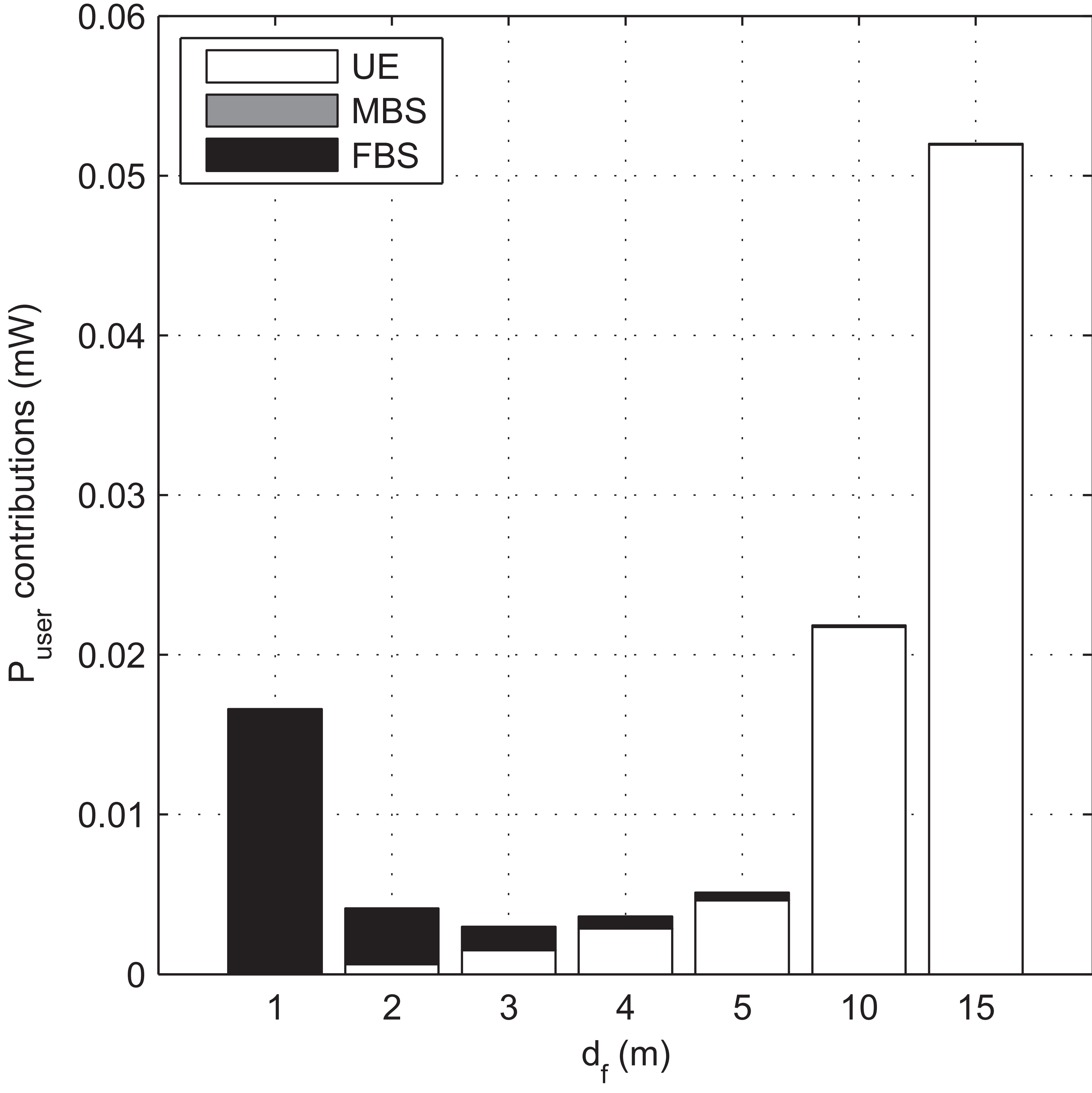

UE
MBS
FBS
0.06
0.05
0.04
0.03
0.02
0.01
0
1
2
3
4
5
10
15
P_{user} contributions (mW)
d_f (m)